International Journal of Modelling and Simulation

ISSN: (Print) (Online) Journal homepage: https://www.tandfonline.com/loi/tjms20

# A numerical optimization study of CdS and Mg0.125Zn0.875O buffer layers in CIGS-based solar cells using *wx*AMPS-1D package.

**Moufdi Hadjab , Jan-Martin Wagner , Fayçal Bouzid , Samah Boudour , Abderrahim Hadj Larbi , Hamza Bennacer , Mohamed Issam Ziane , M A Saeed , Hamza Abid & Smail Berrah**

**To cite this article:** Moufdi Hadjab , Jan-Martin Wagner , Fayçal Bouzid , Samah Boudour , Abderrahim Hadj Larbi , Hamza Bennacer , Mohamed Issam Ziane , M A Saeed , Hamza Abid & Smail Berrah (2020): A numerical optimization study of CdS and Mg0.125Zn0.875O buffer layers in CIGS-based solar cells using *wx*AMPS-1D package., International Journal of Modelling and Simulation, DOI: 10.1080/02286203.2020.1857129

**To link to this article:** https://doi.org/10.1080/02286203.2020.1857129

Published online: 30 Dec 2020.

INTERNATIONAL JOURNAL OF MODELLING AND SIMULATION
https://doi.org/10.1080/02286203.2020.1857129

Taylor & Francis
Taylor & Francis Group

ARTICLE



# A numerical optimization study of CdS and $Mg_{0.125}Zn_{0.875}O$ buffer layers in CIGS-based solar cells using *wx*AMPS-1D package.

Moufdi Hadjab[a], Jan-Martin Wagner[b], Fayçal Bouzid[c], Samah Boudour[c], Abderrahim Hadj Larbi[c], Hamza Bennacer[a], Mohamed Issam Ziane[d], M A Saeed[e], Hamza Abid[f] and Smail Berrah[g]

[a]Electronic Department, Faculty of Technology, Mohamed Boudiaf University of M'sila, M'sila, Algeria; [b]Institute of Materials Science, Technical Faculty, University of Kiel, Kiel, Germany; [c]Research Center in Industrial Technologies CRTI, Cheraga, Algiers, Algeria; [d]École Supérieur En Génie Électrique Et Énergétique d'Oran (ESGEE), Oran, Algeria; [e]Department of Physics, University of Education, Lahore, Pakistan; [f]Applied Materials Laboratory, Research Center, University Djillali Liabes, Sidi Bel Abbes, Algeria; [g]Mastery Renewable Energies Laboratory LMER, University of A. Mira, Bejaia, Algeria

**ABSTRACT**

The performance of copper indium gallium selenium (CIGS) based solar cells with cadmium sulfide (CdS) and magnesium zinc oxide ($Mg_xZn_{1-x}O$) buffer layers has been investigated comparatively with the new version of a one-dimensional device simulation program for the analysis of microelectronic and photonic structures (*wx*AMPS-1D). The structures of solar cells have been analysed keeping in view the effect of doping as well as of thickness of buffer and absorber layers. It is observed that the conversion efficiency and external quantum efficiency (EQE) are improved using $Mg_{0.125}Zn_{0.875}O$ compound buffer layer for ZnO/$Mg_{0.125}Zn_{0.875}O$/CIGS structure to 22.01% and 89.7%, respectively, whereas the obtained conversion efficiency and EQE for ZnO/CdS/CIGS structure are 21.06% and 88.78%, respectively. The obtained results are in good agreement with the recently published work and the proposed structure of solar cells would have potential regarding improvements in the existing solar cell technology.

**ARTICLE HISTORY**
Received 22 November 2020
Accepted 25 November 2020

**KEYWORDS**
Solar cells; buffer layer; *wx*AMPS-1D; conversion efficiency; numerical optimization

## 1. Introduction

In the last two decades, chalcopyrite-type copper indium selenium (CIS) and copper indium gallium selenium (CIGS) are among the most promising and investigated materials to achieve higher efficiency of thin-film solar cells [1] owing to their characteristics, in particular, favourable electronic and optical properties in addition to low-cost fabrication. The national renewable energy laboratory (NREL-USA), the Swiss federal laboratories for material science and technology (EMPA-Switzerland) and the centre of solar energy nd hydrogen research (ZSW-Germany) has reported so far the efficiencies of these solar cells up to 19.9% [2], 20.4% [3], and 22.6% [4], respectively. On the other hand, there are several theoretical reports available in the literature demonstrating the performance of CIGS-based solar cells with efficiencies up to 20.85% [5], and 21.61% [6]. For heterojunction ZnO:$Al_2O_3$(ZAO)/CdS/CIGS thin-film solar cells, efficiencies of 16.39% [7], 19.13% [8], 21.0% [9], 22.3% [10], and 24.35% [11] are reported for using the one-dimensional analysis of microelectronic and photonic structures (AMPS-1D) [12] and the solar cell capacitance simulator (SCAPS-1D) [13] software. Among various other critical parameters that affect the performance of solar cells, thickness and doping of buffer layer between n and p-type active materials play an important role. Conventionally, CIGS-based solar cells have been fabricated with cadmium sulfide (CdS) buffer layer. However, CdS exhibits many electrical, optical, and environmental hindrances due to its toxic nature and there is a lot of chemical waste if used for fabrication of thin films via chemical bath deposition method [14]. Several reports have been published to date regarding investigations on the role of buffer layers of various compounds specifically CdS, zinc sulfide (ZnS), zinc selenide (ZnSe), zinc oxide (ZnO), zinc tin oxide ($Zn_{1-x}Sn_xO$), magnesium zinc oxide ($Mg_xZn_{1-x}O$) and indium selenide ($In_2Se_3$) in flexible CIGS-based solar cells using device emulation program and tool as, e.g., ADEPT 2.1 [15], SCAPS-1D and AMPS-1D numerical simulation packages [16–19]. In the present work, the focus is to employ $Mg_xZn1_{-x}O$ as a buffer layer, which has been identified as a promising Cd-free buffer layer quite early [20] and has shown to be useful in thin-film solar cell applications [21]. The MgZnO buffer layer exhibits higher optical transmittance and is a much more environmental friendly material compared to CdS [14].

**CONTACT** Moufdi Hadjab moufdi.hadjab@univ-msila.dz Electronic Department, Faculty of Technology, Mohamed Boudiaf University of M'sila, M'sila, Algeria

Addition of magnesium (Mg) to ZnO enhances the band-gap energy [22], which leads to a better band alignment with both CIGS absorber and ZnO window layers in solar cells [14].

A number of theoretical studies have been conducted so far to investigate the use of $Mg_xZn_{1-x}O$ buffer layer with different molar fractions of Mg in CIGS solar cells [18,23]. Pettersson et al. [23] reported the study of $Mg_xZn_{1-x}O$ buffer layer with a mole fraction of Mg as 0.17 through the SCAPS-1D software. Pandey et al. [24,25] reported the total conversion efficiencies of 21.4% [24] and 20.8% [25] with MgZnO buffer layer having different mole fraction by commercial technology computer-aided design (TCAD) simulation software. However, the control over appropriate Mg content in $Mg_xZn_{1-x}O$ films is essential to avoid enhanced interface recombination [21]. Therefore, the current work emphasizes on the optimal mole fraction of Mg, and it has been observed that low Mg molar fraction in $Mg_xZn_{1-x}O$, namely $x$ = 0.125, features a suitable band gap value and an excellent absorption coefficient compared to other concentrations reported in the previous work done by M. Hadjab et al. [22]. These characteristics permit to use this material as a buffer layer in the proposed design of solar cells. The package *wx*AMPS-1D [12,26] has been used to study the performance of CIGS-based thin-film solar cells with standard CdS and proposed $Mg_{0.125}Zn_{0.875}O$ buffer layer. The influence of doping concentration along with the thickness of the absorber layer for both ZnO/n-CdS/p-CIGS and ZnO/n-$Mg_{0.125}Zn_{0.875}O$/p-CIGS solar cells has been investigated.

## 2. Device structures and simulation parameters

The transport physics in thin-film solar cell structures can be investigated by one-dimensional AMPS software package [12,27,28]. AMPS-1D solves the Poisson's equation with six boundary conditions and equations of electron-hole continuity by the Newton–Raphson and finite difference approach. The numerical simulation has been carried out through implanting the density of states (DOS) model [29,30]. A highly stable freeware solar cell simulation program *wx*AMPS-1D is an enhanced version of the original AMPS-1D program. It was designed by the University of Illinois at Urbana–Champaign (UIUC), in collaboration with Nankai University of China by Y. Liu et al. [26] according to the physical principles of AMPS-1D software tool developed at Pennsylvania State University by S. Fonash et al. [12]. The package *wx*AMPS-1D is written in C++ Language with a number of modifications in basic algorithms, namely, it uses the fundamental physical principles of AMPS-1D, includes portion tunnelling currents to the model, delivers an improved visualisation and, improves convergence and execution speed [26]. The modified algorithm was solved by combining the Newton and Gummel approximations with a better stability, speed, and effectiveness. *wx*AMPS-1D is similar in performance to SCAPS-1D but provides better ability to model materials with high defect densities, band tails, and other features typical of thin-film solar cells [26]. Furthermore, with an accurate setting of the input parameters, it is possible to study the optical responses and electrical transport phenomena of the solar cell structures [31].

The main equations used by *wx*AMPS-1D to describe the solid-state device are given below:

$$\frac{d}{dx}\left(-\varepsilon(x)\frac{d(\phi)}{dx}\right) = q\rho \tag{1}$$

$$\frac{1}{q}\frac{dJ_n}{dx} = R_n(x) - G(x) \tag{2}$$

$$\frac{1}{q}\frac{dJ_p}{dx} = G(x) - R_p(x) \tag{3}$$

$$J_n(x) = q\mu_n n\left(\frac{dE_{fn}}{dx}\right) \tag{4}$$

$$J_p(x) = q\mu_p n\left(\frac{dE_{fp}}{dx}\right) \tag{5}$$

Equation (1) is the Poisson's equation, where $x$ is position (device length), $\varepsilon$ is dielectric constant, $\varphi$ is local electrostatic potential, as well as the elementary charge $q$ and total charge density $\rho$. Equations (2) and (3) are the equations of continuity for electrons and holes, respectively. The terms $J_n$ and $J_p$ correspond to the electron and hole current densities, respectively. $R_n(x)$, $R_p(x)$ are the electrons' and holes' recombination rates. $G(x)$ is termed as optical carrier generation rate that depends on external illumination. Equations (4) and (5) are general relations to access motion of charge carriers due to diffusion and drift phenomenon under the influence of effective fields arising from band gap, electron affinity, and densities-of-states gradients. Here, $\mu_n$ and $\mu_p$ are the electron and hole mobility, respectively [32].

As it was mentioned above, *wx*AMPS-1D computer program simulator is a freeware, which is utilized to emulate a real thin-film solar cell's performance. The numerical simulation was carried through the following steps shown in figure 1 as screenshots. The screenshot (a) shows the *wx*AMPS-1D main input panel graphical user

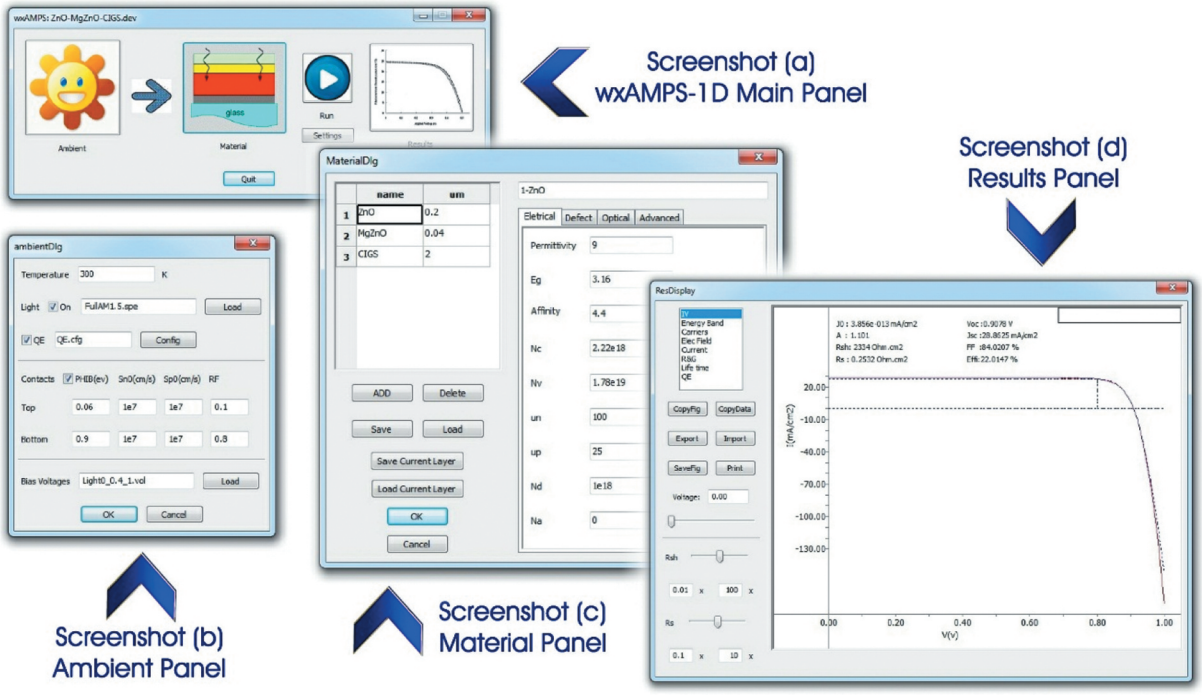


**Figure 1.** Data input panels of *wx*AMPS-1D graphical user interface used for setting up the parameters for optimization of solar cell.

interface for the numerical simulation process of thin-films solar cells. The main input panel consists of four panels, as follows: the ambient panel in which solar cells determine an appropriate working environment, the input material panel, the input settings panel, and finally the output panel illustrating the simulation results. The

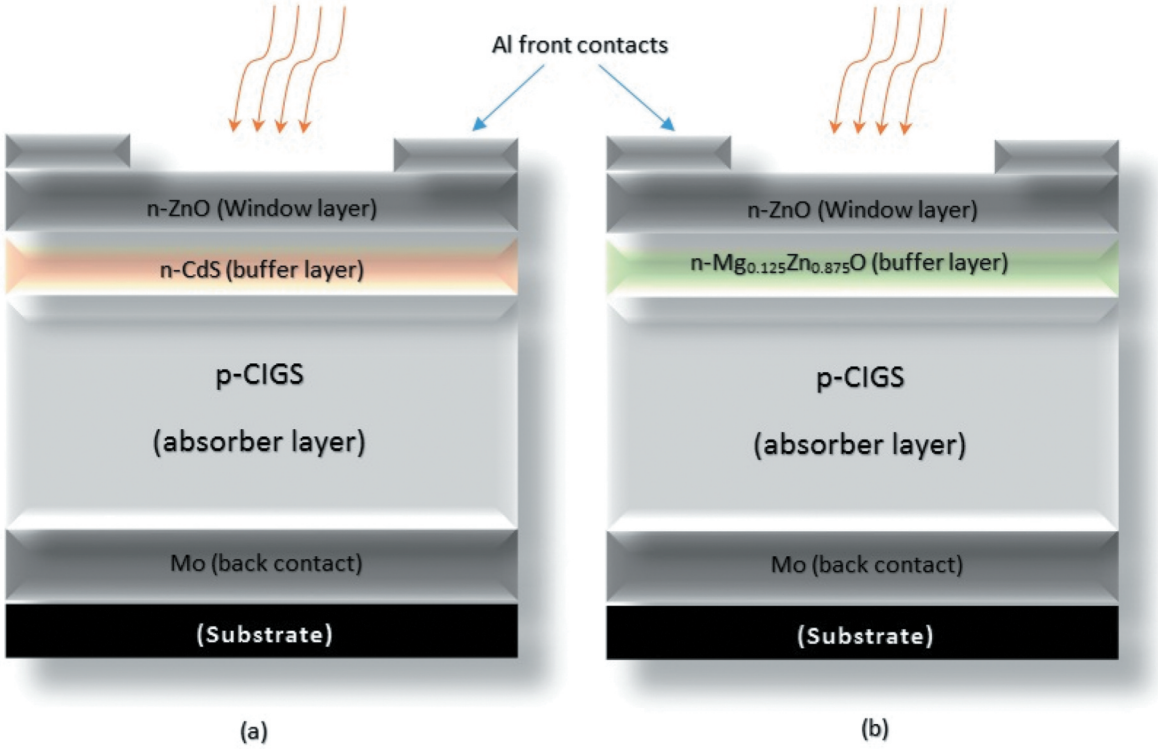


**Figure 2.** Schematic cross-sections of the two CIGS-based thin-film solar cells: (a) with CdS buffer layer; (b) with $Mg_{0.125}Zn_{0.875}O$ buffer layer.

screenshot (b) shows the biasing conditions for the solar cell (temperature and light bias defined by the spectrum and flux), the contact parameters (thermal velocity recombination for holes/electrons, potential barrier height, and reflectivity at the front and back contacts) as well as the bias voltages as defined by the user. The screenshot (c) shows the device definition, *i.e.* solar cell structure design, and the selection of material for each layer, as well as the input electrical/optical properties (e.g. permittivity, bandgap, affinity, the effective density of states, doping, mobilities, defect distribution at the interfaces, etc). Finally, the results of J-V characteristics; conversion efficiency (η), fill factor (FF), short-circuit current density ($J_{sc}$), and open-circuit voltage ($V_{oc}$) can be visualized as curves via panel shown in the screenshot (d).

In the present work, CIGS-based solar cells consisted of a set of layers in the following order from top-to-bottom: (a) Al front contact/ZnO window/n-CdS buffer/p-CIGS absorber/Mo back contact; (b) Al front contact/ZnO window/n-$Mg_{0.125}Zn_{0.875}O$ buffer/p-CIGS absorber/Mo back contact has been studied as shown in figure 2. It was assumed that most of the incident photons would pass through the window layer then the buffer layers, and finally, the absorber layer of the cell structure will absorb them. The schematic band diagrams of the structures, under illumination, are shown in figure 3. The key parts of both cell structures are CIGS absorber and the two different buffer layers (CdS and $Mg_{0.125}Zn_{0.875}O$). The ZnO window, owing to its wide bandgap, serves as transparent conductive oxide (TCO). The input parameters used for the simulation of both structures are summarized in table 1. These parameters include thickness, relative permittivity, electron affinity, optical band gap, electron/hole mobility, donor/acceptor concentrations, and effective density of states in both conduction and valance bands (CB, VB). The value of bandgap energy of 3.33 eV for $Mg_{0.125}Zn_{0.875}O$ buffer layer has been obtained from first-principles calculations using the full potential linearized augmented plane wave (FP-LAPW) calculations based on density functional theory (DFT) [22]. When illuminating the two devices, photons with energy lower than 3.16 eV have wavelengths greater than the cutoff wavelength of ZnO (0.393 μm) and will pass through the ZnO window layer. In contrast, each layer absorbs photons having shorter wavelengths than its own cutoff wavelength, where the cutoff wavelengths of CdS, $Mg_{0.125}Zn_{0.875}O$ and CIGS are 0.517, 0.372, and 0.886 μm, respectively.

## 3. Results and discussion

Performance analysis and determination of the tradeoff between the two designs as shown in figure 2 have been carried out by investigating the effect of thickness and doping of both the layers *i.e.* absorber and buffer layer especially on the photovoltaic (PV) parameters, by simulation of characteristics like current density-voltage, power density-voltage, and quantum efficiency. The simulation has been performed using the air mass 1.5 global spectral irradiance data (AM1.5 G, 1000 $W/m^2$) at room temperature (300 K).

### 3.1 Influence of the doping concentration in n-CdS and n-$Mg_{0.125}Zn_{0.875}O$ buffer layers

The thickness of CdS and $Mg_{0.125}Zn_{0.875}O$ buffer layers was taken as 50 and 40 nm, respectively, while the doping concentration was varied in the range $1.0 \times 10^{15}$ to $1.0 \times 10^{17}$ $cm^{-3}$ for CdS and $1 \times 10^{15}$ to $4.0 \times 10^{17}$ $cm^{-3}$ for $Mg_{0.125}Zn_{0.875}O$. The PV parameters η, FF, $J_{sc}$, and $V_{oc}$ have been extracted as a function of donor doping concentration ($N_D$) of the buffer layer and represented in figure 4. Simulation results suggest that the η, FF of the two different structures of solar cells increases progressively with the doping concentration of buffer layer and reaches a maximum value as η = 21.06%, FF = 82.75%, and η = 22.01%, FF = 84.02% for CdS and $Mg_{0.125}Zn_{0.875}O$, respectively. The optimized donor concentrations for buffer layers are found to be $N_D(CdS) = 6.3 \times 10^{16}$ $cm^{-3}$ and $N_D(Mg_{0.125}Zn_{0.875}O) = 2.5 \times 10^{17}$ $cm^{-3}$. These considerable enhancements in η and FF resulted from the well-known solar PV theory that demonstrates that an increment in the concentration of donor atoms of emitter increases the concentration of the photo-generated carriers under illumination; hence, improving the collection of charge carriers that leads to an enhanced short-circuit current density as shown in figure 4 -c. This observation is inconsistent with the results reported earlier [33]. Moreover, the simulation results reveal that the increase in $N_D$ has a little effect on the open-circuit voltage $V_{oc}$ as shown in figure 4 -d.The observed decline of $V_{oc}$ could be due to the decrease of the saturation current caused by the reduction in diffusion length and diminution of the carrier's mobility.

### 3.2 Effect of thickness of CdS and $Mg_{0.125}Zn_{0.875}O$ buffer layers

Let us now turn our attention to the effect of the buffer layer thickness on the solar cell performance. For that, we are going to illustrate the variation of the cell parameters versus a CdS and $Mg_{0.125}Zn_{0.875}O$ buffer layer thickness ranging from 20 to 500 nm, as shown in figure 5. The best performance of solar cell structures for both structures is found for a buffer layer thickness of 50 and 40 nm for CdS

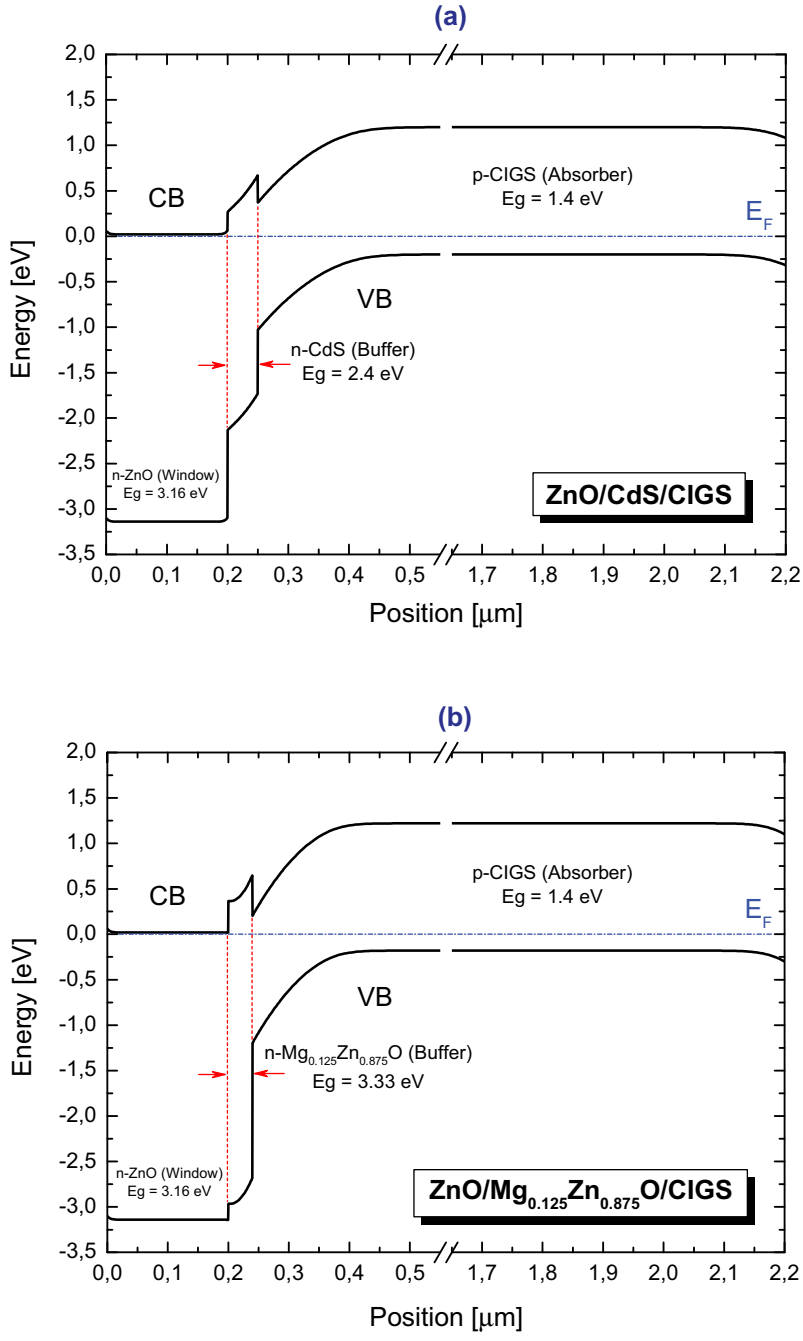


**Figure 3.** Energy band diagrams of solar cells obtained from *wx*AMPS-1D software: (a) ZnO/n-CdS/p-CIGS and (b) ZnO/n-$Mg_{0.125}Zn_{0.875}O$/p-CIGS.

and $Mg_{0.125}Zn_{0.875}O$, respectively. These values have been chosen in order to provide the highest conversion efficiency. The PV parameters of the solar cells drop slightly since a small number of photons approaches the absorber layer. The same behaviour has already been reported in the previous studies [5,11,31]. Consequently, it is desirable to reduce the buffer layer thickness in order to minimize the optical absorption losses.

### 3.3 Influence of the doping concentration in p-CIGS absorber layer

In order to find out the optimal doping and thickness of the p-CIGS region (figure 6), which corresponds to the most efficient location for absorption, the PV parameters of the two solar cell structures have been simulated in terms of the doping concentration of acceptors ($N_A$) in the range $1.0 \times 10^{15}$ to $1.25 \times 10^{17}$ $cm^{-3}$ with a thickness of 2.0 µm for both CIGS-based solar cell structures.

**Table 1.** Parameters used for the *wx*AMPS-1D simulations.

| Layer properties | n- ZnO | n-CdS | n-$Mg_{0.125}Zn_{0.875}O$ | p-CIGS |
|---|---|---|---|---|
| Thickness [nm] | 200[9] | Variable | Variable | Variable |
| Relative permittivity, $\varepsilon_r$ | 9[6,9] | 10[5,9] | 10.5[24,25] | 13.6[5,9] |
| Electron affinity, $\chi$ [eV] | 4.4[9] | 4.2[9] | 4.05[24,25] | 4.5[5,10] |
| Optical band gap, $E_G$ [eV] | 3.16[22] | 2.4[6] | 3.33[22] | 1.4 *[9,34,37] |
| Electron mobility, $\mu_n$ [$cm^2$/Vs] | 100[6,10] | 100[5,10] | 300[24,25] | 100[5,10] |
| Hole mobility, $\mu_p$ [$cm^2$/Vs] | 25[6,10] | 25[5,10] | 20[24,25] | 25[5,10] |
| Effective density of states in the conduction band, $N_C$ [$cm^{-3}$] | $2.22 \times 10^{18}$[6] | $2.22 \times 10^{18}$[6] | $2.22 \times 10^{18}$[24,25] | $2.22 \times 10^{18}$[6] |
| Effective density of states in the valance band, $N_V$ [$cm^{-3}$] | $1.78 \times 10^{19}$[6] | $1.78 \times 10^{19}$[6] | $1.78 \times 10^{19}$[24,25] | $1.78 \times 10^{19}$[6] |
| Acceptor concentration, $N_A$ [$cm^{-3}$] | 0[10,27] | 0[10,27] | 0[24,25] | Variable |
| Donor concentration, $N_D$ [$cm^{-3}$] | $1 \times 10^{18}$[10] | Variable | Variable | 0[10,27] |
| **General device properties** | **Front Surface** | | **Back Surface** | |
| Reflectance (RF) | 0.1 [35,37] | | 0.8 [35,37,38] | |
| Work function of metal contacts $\Phi b_{0/L} = PHIB_{0/L} = E_C - E_F$ [eV] | 0.06 eV[34] | | 0.9[6,34,39] | |
| Recombination velocity for holes [m/s] | $10^7$[5,35,37] | | $10^7$[5,35] | |
| Recombination velocity for electrons [m/s] | $10^7$[5,35,37] | | $10^7$[5,35] | |

* The value of 1.4 eV is taken for $x = 0.6$ for $CuIn_xGa_{1-x}Se_2$ [9,34,37]

It has been observed that η increases progressively with increasing the doping concentration in both solar cell structures, approaches a maximum value, and then decreases gradually for further increase in doping concentration. More precisely, in case of the ZnO/MgZnO/CIGS structure (see figure 6 -a), when the doping concentration increases from $1.0 \times 10^{15}$ to $5.2 \times 10^{16}$ $cm^{-3}$, η increases from 18.5% to 22%; afterwards, it begins to decrease gradually from $6.0 \times 10^{16}$ $cm^{-3}$ for further increase in doping concentration. On the other hand, in case of ZnO/CdS/CIGS structure (see figure 6 -a), for doping concentration that changes from $1.0 \times 10^{15}$ to $2.9 \times 10^{16}$ $cm^{-3}$, η increases from 18% to 21%; after that, it decreases gradually from $3.0 \times 10^{16}$ $cm^{-3}$ for further increase in doping concentration. These observations are in good agreement with the previous reports [6,33]. Keeping in view the fact that with increasing the acceptor concentration in the absorber layer, saturation current density decreases, which leads to enhance the open-circuit voltage $V_{oc}$. However, as the doping increases and reaches ever-higher levels, the depletion region between the buffer and absorber layers narrows, ensuing a declining trend of total charge carriers collected, photocurrent intensity, and the short-circuit current density as shown in figure 6 -c. The high performance of PV cells have been reached at the absorber layer doping concentration value of $5.2 \times 10^{16}$ $cm^{-3}$ and $2.9 \times 10^{16}$ $cm^{-3}$ for ZnO/MgZnO/CIGS and ZnO/CdS/CIGS, respectively.

### 3.4 Effect of thickness of CIGS absorber layer

The effect of thickness of the CIGS absorber layer on the output electrical parameters of the two solar cells has also been predicted as shown in figure 7. At first glance, after an overview of the data shown in figure 7, it can be observed that, as the thickness of the p-CIGS absorber layer increases, the solar cell efficiency improves rapidly and saturates gradually for thicknesses exceeding 2000 nm. The conversion efficiency changes, respectively, from 14.30% to 21.06% and from 15.80% to 22.01%, for both studied solar cells ZnO/CdS/CIGS and ZnO/MgZnO/CIGS, as a function of absorber layer thickness. The improvement in η is due to the fact that an absorber layer with an optimal thickness leads to the maximum absorption of photons with a wide range of wavelengths (figure 8) that consequently enhances the short-circuit current and open-circuit voltage. The best performance of solar cells have been achieved when the absorber layer thickness is around 1.8 to 2.5 μm (figure 7 -a). However, from a practical point of view, at a thickness of 2.0 μm, the performance is quite close to the optimal value. The same trend has been observed for all solar cell parameters like η, FF, $J_{sc}$, and $V_{oc}$ under-optimized simulation conditions. figures 6 and 7 reveal that the cell structure with n-$Mg_{0.125}Zn_{0.875}O$ buffer layer illustrates a better performance with η = 22.01%, FF = 84.02%, $J_{sc}$ = 28.76 mA/$cm^2$, and $V_{oc}$ = 0.90 V, compared to the cell structure with n-CdS buffer layer with η = 21.06%, FF = 82.61%, $J_{sc}$ = 28.75 mA/$cm^2$, and $V_{oc}$ = 0.88 V. These simulation results shows that the $Mg_{0.125}Zn_{0.875}O$ buffer layers may serve as a viable substitute for CdS in solar cells. Almost the same behaviour has already seen in the previous studies [5–7,17,25,31,34]

### 3.5 Effect of thickness of CIGS absorber layer on the EQE

Figure 8 shows the EQE [19], also called spectral response (SR), which is current per unit flux for each bandwidth as a function of the absorber layer thickness. It is evident from figure 8 that the EQE has the

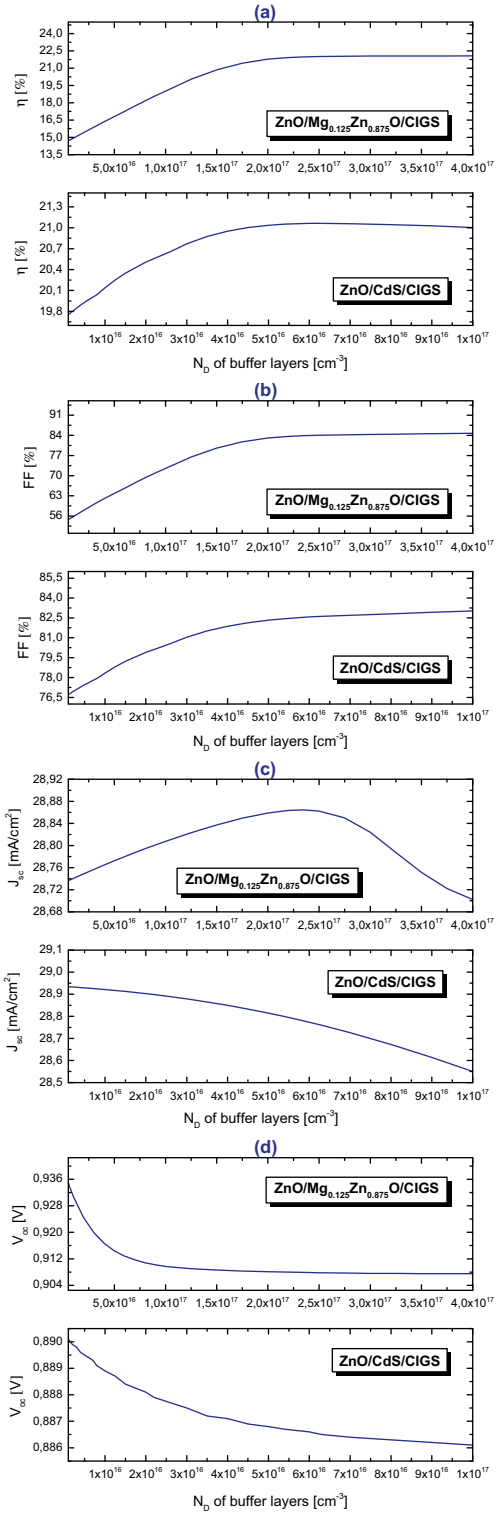


**Figure 4.** The output parameters (a) η, (b) FF, (c) $J_{sc}$ and (d) $V_{oc}$ as a function of buffer layer doping for ZnO/n-CdS/p-CIGS and ZnO/n-$Mg_{0.125}Zn_{0.875}O$/p-CIGS solar cells.

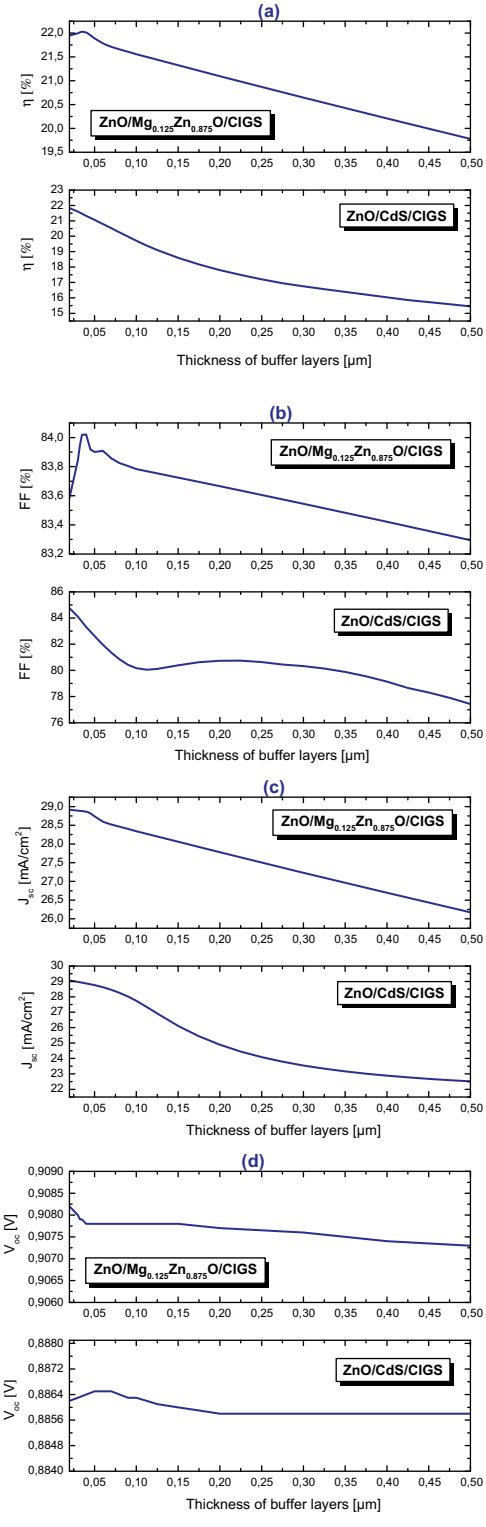


**Figure 5.** The output parameters (a) η, (b) FF, (c) $J_{sc}$ and (d) $V_{oc}$ as a function of buffer layer thickness for ZnO/n-CdS/p-CIGS and ZnO/n-$Mg_{0.125}Zn_{0.875}O$/p-CIGS solar cells.

maximum values of 88.78% at 540 nm and 89.7% at 440 nm (for 2.0 μm thick p-CIGS) for ZnO/n-CdS/p-CIGS and ZnO/n-$Mg_{0.125}Zn_{0.875}O$/p-CIGS, respectively. The drop at higher wavelengths (~ 885 nm) corresponds to the CIGS band gap ($E_G$ = 1.4 eV).

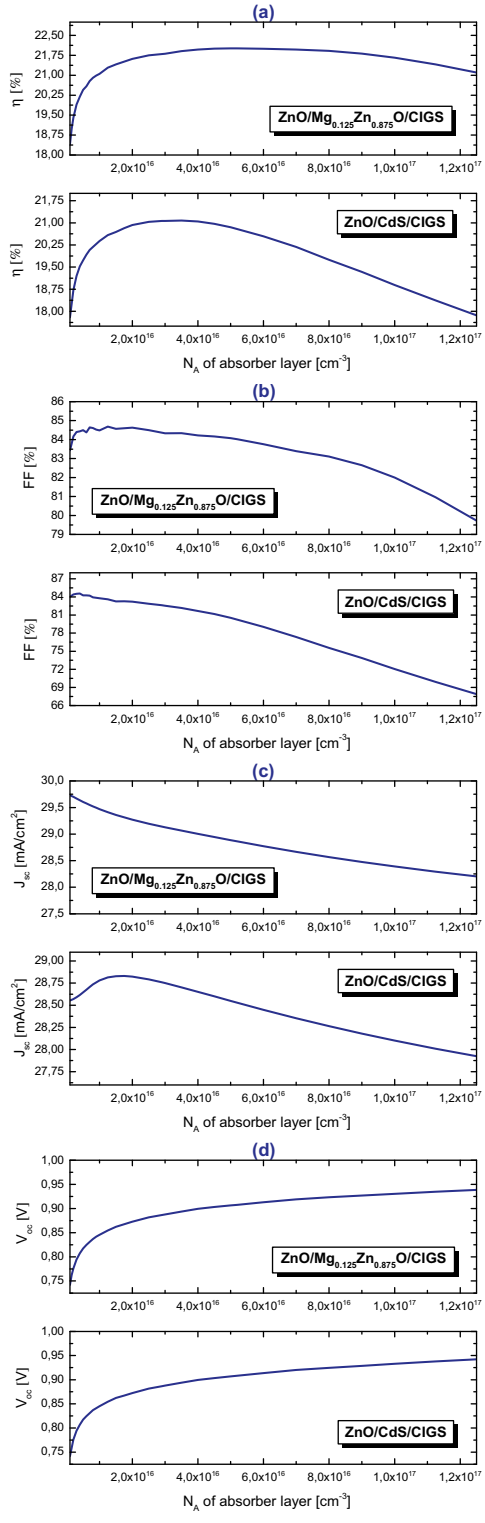


**Figure 6.** The output parameters (a) η, (b) FF, (c) $J_{sc}$ and (d) $V_{oc}$ as a function of absorber layer doping for ZnO/n-CdS/p-CIGS and ZnO/n-$Mg_{0.125}Zn_{0.875}O$/p-CIGS solar cells.

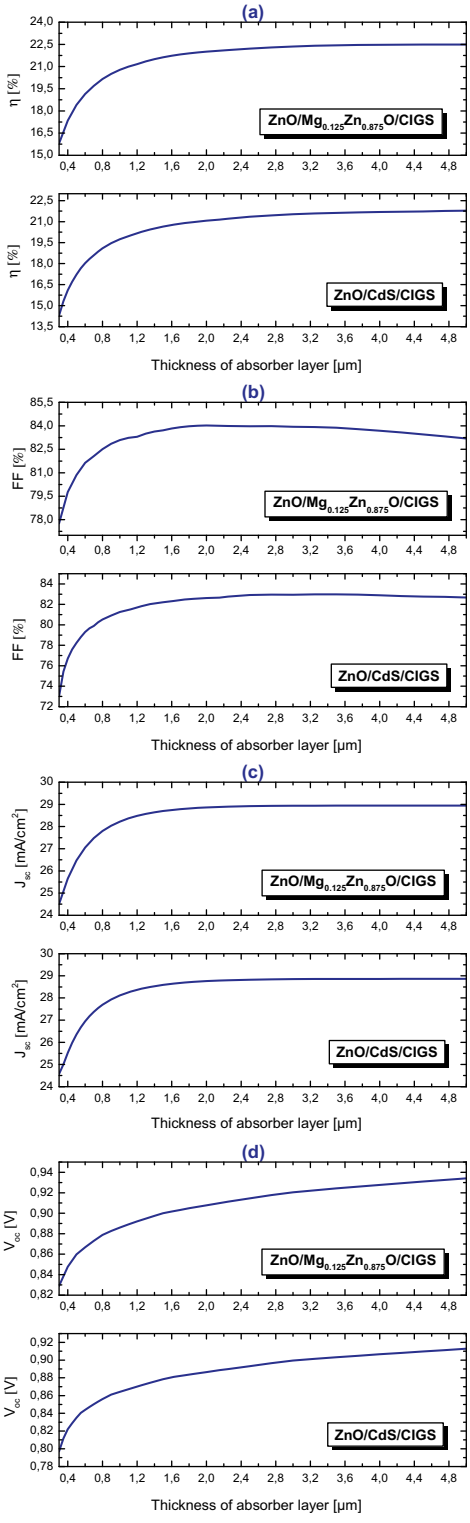


**Figure 7.** The output parameters (a) η, (b) FF, (c) $J_{sc}$ and (d) $V_{oc}$, as a function of the p-CIGS absorber thickness for ZnO/n-CdS/p-CIGS and ZnO/n-$Mg_{0.125}Zn_{0.875}O$/p-CIGS solar cells.

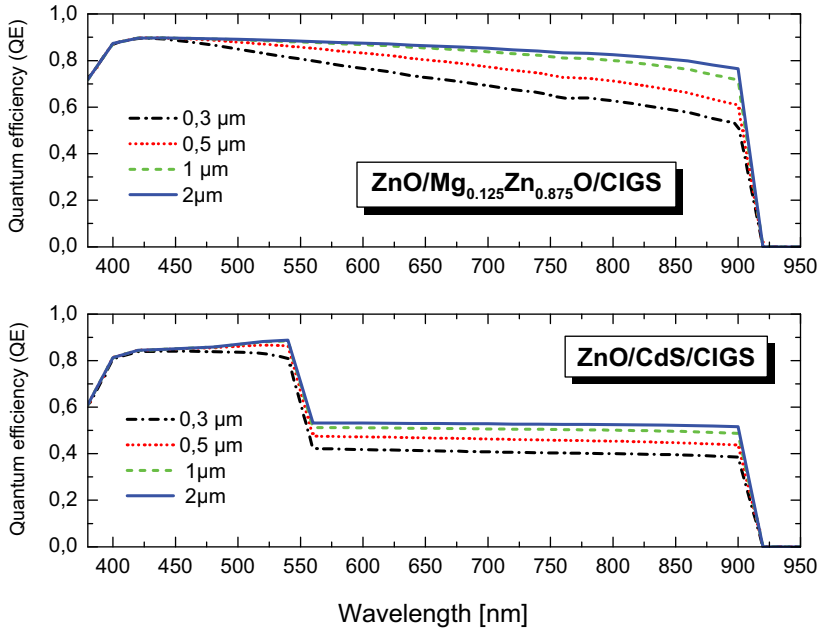


**Figure 8.** The simulated external quantum efficiency as a function of wavelength, at various thicknesses of the p-CIGS absorber layer for ZnO/n-CdS/p-CIGS and ZnO/n-$Mg_{0.125}Zn_{0.875}O$/p-CIGS solar cells.

### *3.6 Effect of thickness of CIGS absorber layer on the J-V and P-V characteristics*

In the same context, and in order to evaluate the rate of change of output parameters of CIGS thin-film solar cells with different thicknesses of absorber layer, current-density voltage characteristic J(V) have been simulated under illumination as shown in figure 9. It can be observed from figure 9 that both the short-circuit current and open-circuit voltage increases as a function of absorber layer thickness, which leads to an increase in the other two PV parameters (η and FF), as well as the maximum-delivered power as shown by the power-density voltage characteristic P(V) in figure 10.

As reported in figure 9, the simulated curves disclose that the variation in absorber layer thickness from 300

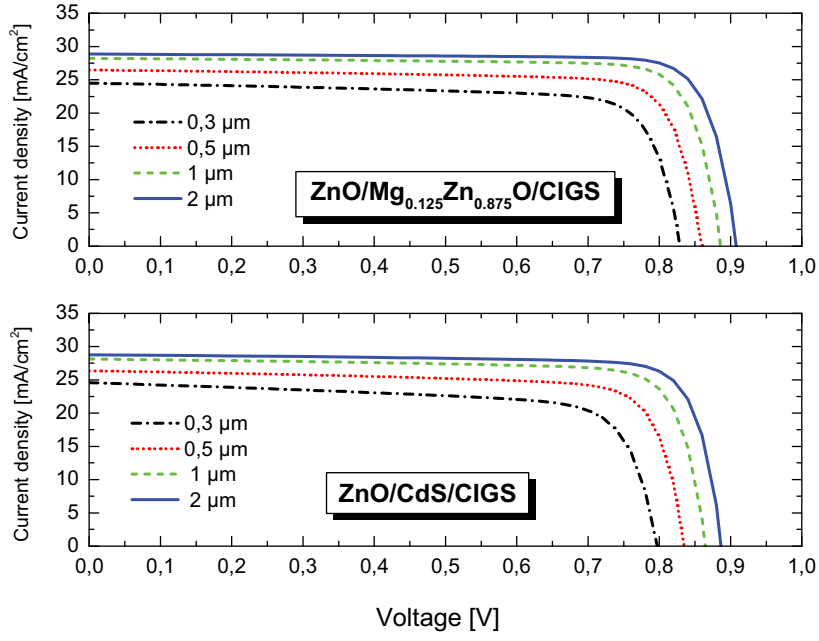


**Figure 9.** Simulated J(V) characteristics, for different p-CIGS absorber thicknesses, of ZnO/n-CdS/p-CIGS and ZnO/n-$Mg_{0.125}Zn_{0.875}O$/p-CIGS solar cells.

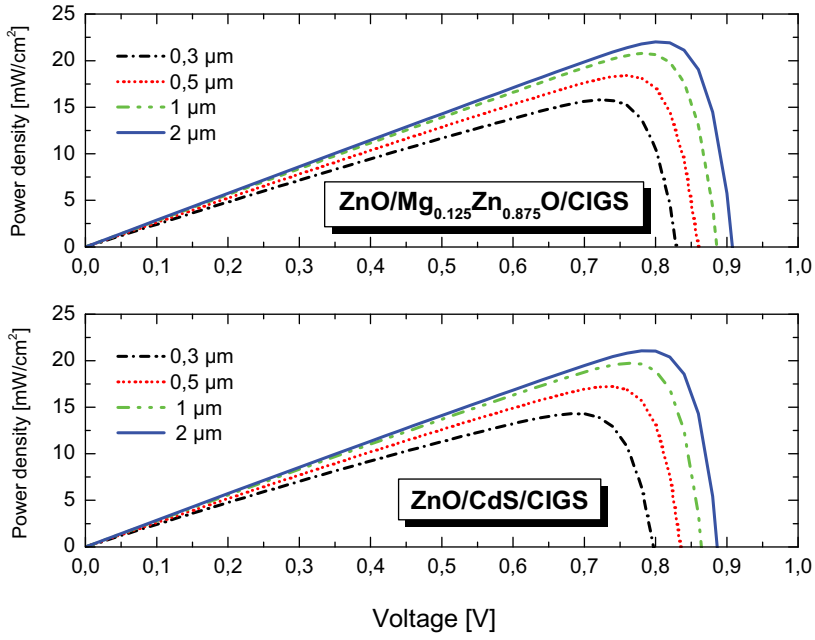


**Figure 10.** Simulated P(V) characteristics, for different p-CIGS absorber thickness thicknesses, of ZnO/n-CdS/p-CIGS and ZnO/n-$Mg_{0.125}Zn_{0.875}O$/p-CIGS solar cells.

to 2000 nm improves the η, FF, $J_{sc}$, and $V_{oc}$ by 32.07%, 11.60%, 14.54%, and 10.08%, respectively, for the cell structure based on the CdS buffer layer. Nevertheless, for the second cell structure that is based on $Mg_{0.125}Zn_{0.875}O$ buffer layer, the proportions of improvement in η, FF, $J_{sc}$, and $V_{oc}$ are found as 28.21%, 7.44%, 15.08%, and 8.67%, respectively. This improvement in output parameters of the studied structures with higher thickness of absorber layer is justified since the maximum-absorbed photons quantity with longer wavelengths would result in the collection of higher photogenerated carriers.

Figure 10 shows a considerable improvement in the maximum output power density from 14.30 to 21.06 mW/cm$^2$ for ZnO/CdS/CIGS solar cell as the thickness of absorber layer varies from 0.3 to 2.0 µm. However, for the second solar cell structure, the maximum output power density is optimized from 15.80 to 22.01 mW/cm$^2$ as the thickness of the absorber layer varies from 0.3 to 2.0 µm. Table 2 summarizes the results of numerical simulation including η, FF, $J_{sc}$, and $V_{oc}$.

### 3.7 Optimal J-V and P-V characteristics

By using the optimized parameters of both ZnO/n-CdS/p-CIGS and ZnO/n-$Mg_{0.125}Zn_{0.875}O$/p-CIGS thin-film solar cell structures, the simulated J-V characteristics and the corresponding-extracted output parameters as

**Table 2.** Comparison of output parameters of the optimized thin-film solar cell structures with already reported theoretical and experimental findings.

| CIGS-based structures | | Thicknesses (nm) | | | | η [%] | FF [%] | $J_{sc}$ [mA/cm$^2$] | $V_{oc}$ [V] |
|---|---|---|---|---|---|---|---|---|---|
| | | **n-ZnO** | **n-CdS** | **n-MgZnO** | **p-CIGS** | | | | |
| **ZnO/MgZnO/CIGS** | **Our work** | **200** | | **40** | **2000** | **22.01** | **84.02** | **28.86** | **0.90** |
| | Ref. [24] | - | | 300 | 1000 | 21.4 | 85.7 | 34.8 | 1.2 |
| | Ref. [25] | 50 | | 300 | 1000 | 20.8 | 84.7 | 33.5 | 0.95 |
| **ZnO/CdS/CIGS** | **Our work** | **200** | **50** | | **2000** | **21.06** | **82.61** | **28.75** | **0.88** |
| | Ref. [2] | - | - | | 2200 | 19.9 | 81.2 | 35.5 | 0.69 |
| | Ref. [3] | - | - | | - | 20.4 | 78.9 | 35.1 | 0.73 |
| | Ref. [5] | - | 50 | | 3000 | 20.85 | 82.93 | 36.19 | 0.69 |
| | Ref. [6] | 50 | 100 | | 2500 | 21.61 | 70.0 | 34.10 | 0.90 |
| | Ref. [7] | 20 | 50 | | 1000 | 16.39 | 81.38 | 32.82 | 0.61 |
| | Ref. [38] | 200 | 50 | | 3000 | 17.7 | 79.5 | 34.6 | 0.64 |
| | Ref. [40] | 400 | 50 | | 2000 | 19.04 | 78.9 | 35.23 | 0.68 |
| | Ref. [41] | 200 | 50 | | 3000 | 19.88 | 80.22 | 36.4 | 0.68 |
| | Ref. [35] | 200 | 50 | | 3000 | 24.27 | 85.73 | 33.09 | 0.85 |
| | Ref. [34] | 60 | 40 | | 1000 | 21.44 | 85.1 | 29.56 | 0.85 |

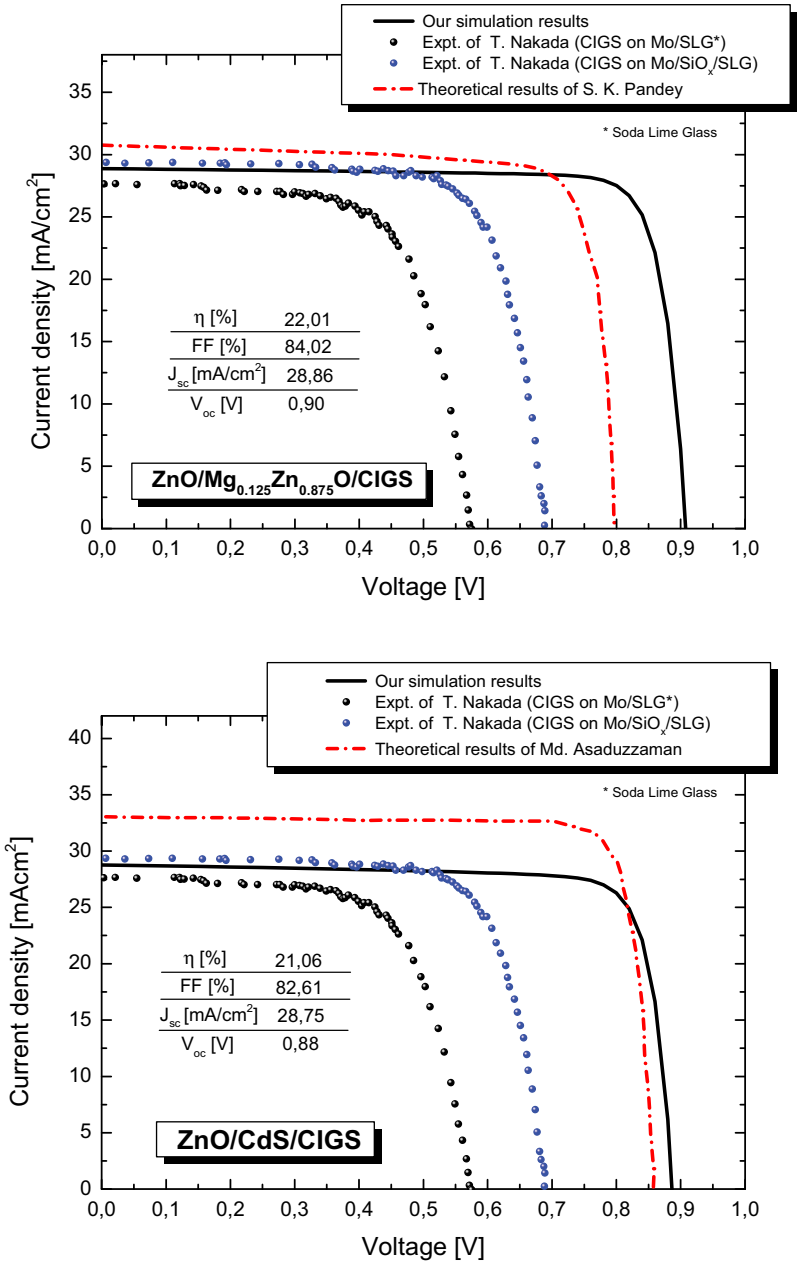


**Figure 11.** Simulated J–V characteristics compared with the theoretical [24,35] and experimental [36] works, for ZnO/n-CdS/p-CIGS and ZnO/n-$Mg_{0.125}Zn_{0.875}O$/p-CIGS thin-films solar cells.

shown in figure 11. The findings are compared and validated with the previously reported theoretical [24,35] and experimental [36] data for ZnO/n-CdS/p-CIGS and ZnO/n-$Mg_{0.125}Zn_{0.875}O$/p-CIGS thin-films solar cell structures.

It has been observed that the solar cell with $Mg_{0.125}Zn_{0.875}O$ buffer layer demonstrated the optimal performance *i.e.* $\eta = 22.01\%$, FF = 84.02%, $J_{sc} = 28.86$ mA/cm$^2$ and $V_{oc} = 0.90$ V, compared with ZnO/CdS/CIGS cell which gives $\eta = 21.06\%$, FF = 82.61%, $J_{sc} = 28.75$ mA/cm$^2$, and $V_{oc} = 0.88$ V. The relative difference between these two solar cell structures is observed to be 4.31%, 1.66%, 0.35%, and 2.34% for η, FF, $J_{sc}$, and $V_{oc}$, respectively.

## 4. Conclusion

Based on the previous work [22] regarding a better absorption coefficient of $Mg_{0.125}Zn_{0.875}O$ compound, the performance of CIGS-based solar cell has been compared with that having CdS compound, using the *wx*AMPS-1D computational package. The performance of two different solar cell structures have been

optimized and compared in terms of doping and thickness of buffer and absorbing layers, under AM 1.5 G illumination. The best performance parameters are found for n-$Mg_{0.125}Zn_{0.875}O$ buffer layer (η = 22.01%, FF = 84.02%, $J_{sc}$ = 28.86 mA/cm$^2$, and $V_{oc}$ = 0.90 V). Therefore, $Mg_{0.125}Zn_{0.875}O$ alloy could serve as a better viable replacement for the standard CdS buffer layer in CIGS thin-film solar cells. Overall, the findings are of great significance to enable technological improvement in the future experimental work.

## Acknowledgments

We acknowledge the use of *wx*AMPS-1D program developed by Dr. Fonash's group of Pennsylvania State University and Dr. Yiming Liu of the University of Illinois at Urbana–Champaign.

## Disclosure statement

No, potential conflict of interest was reported by the authors.

## Notes on contributors

***Dr. Moufdi Hadjab*** is a teacher-researcher at the Electronic Department, University Mohamed Boudiaf of M'Sila. He is working on organic/inorganic solar cells, Density Functional Theory/ Molecular Dynamics simulation of Micro/ Optoelectronics materials and devices.

***Dr. Jan-Martin Wagner*** is at Kiel University (CAU) where he joined J. Carstensen to do CELLO investigations and luminescence measurements (both EL and PL). Presently, his work focuses on the distributed character of the series resistance, both from the theoretical and the experimental point of view.

***Dr. Fayçal Bouzid*** is a researcher at Thin Films Development and Applications Unit – Setif attached with National Center in Industrial Technologies CRTI. Presently he is working on thin films solar cells.

***Dr. Samah Boudour*** is a researcher at Thin Films Development and Applications Unit – Setif attached with National Center in Industrial Technologies CRTI. She is working on thin films solar cells.

***Dr. Abderrahim Hadj Larbi*** is a researcher at Thin Films Development and Applications Unit – Setif attached with National Center in Industrial Technologies CRTI. He is working on the physical properties of materials for nuclear applications.

***Dr. Hamza Bennacer*** is a teacher-researcher at the Electronic Department, University Mohamed Boudiaf of M'Sila. He is working on thin films solar cells, Density Functional Theory of semiconductors materials and opto-electronic devices.

***Dr. Mohamed Issam Ziane*** is a teacher at theHigher School of Electrical and Energy Engineering of Oran. He is working on fundamental properties of materials for micro-electronics applications.

***Prof. Dr. M A Saeed*** is a scientist at the Department of Physics, University of Education, Lahore in Pakistan. He is working generally on the applied physics .

***Prof. Hamza Abid*** is a teacher-researcher at Djillali Liabes University of Sidi Bel Abbes. He is working on the semiconductors alloys within DFT framework.

***Prof. Smail Berrah*** is a teacher-researcher at A/Mira University of Bejaia. He is working on the semiconductors alloys for telecommunication applications.

## ORCID

Moufdi Hadjab http://orcid.org/0000-0001-5595-3317

## References

[1] Arbouz H, Aissat A, Vilcot JP. Simulation and optimization of CdS-n/$Cu_2ZnSnS_4$ structure for solar cell applications. Int J Hydrogen Energ. 2017;42(13):8827.
[2] Repins I, Contreras MA, Egaas B, et al. 19·9%-efficient ZnO/CdS/$CuInGaSe_2$ solar cell with 81·$_2$% fill factor. Prog Photovolt Res Appl. 2008;16(3):235.
[3] Chirilă A, Reinhard P, Pianezzi F, et al. Potassium-induced surface modification of Cu(In,Ga)$Se_2$ thin films for high-efficiency solar cells. Nat Mater. 2013;12 (12):1107.
[4] Jackson P, Wuerz R, Hariskos D, et al. Effects of heavy alkali elements in Cu(In,Ga)$Se_2$ solar cells with efficiencies up to $_{22}$.6%. Phys Status Solidi Rapid Res Lett. 2016;10(8):583. .
[5] Benmir A, Aida MS. Analytical modeling and simulation of CIGS solar cells. Enrgy Proced. 2013;36:618.
[6] Bhuiyan MAM, Islam MS, Datta AJ. Modeling, simulation and optimization of high performance CIGS solar cell. Int J Comput Appl. 2012;57(16):26.
[7] Heriche H, Rouabah Z, Bouarissa N. New ultra thin CIGS structure solar cells using SCAPS simulation program. Int J Hydrogen Energ. 2017;42(15):9524.
[8] Arbouz H, Aissat A, Vilcot JP. Modeling and optimization of CdS/$CuIn_{1-x}Ga_xSe_2$ structure for solar cells applications. Int J Hydrogen Energ. 2016;41(45):20987.
[9] Parisi A, Pernice R, Rocca V, et al. Graded carrier concentration absorber profile for high efficiency CIGS solar cells. Int J Photoenergy. 2015;2015:410549.
[10] Chen W, Huang X, Cheng Q, et al. Simulation analysis of heterojunction ZnO/CdS/Cu(In,Ga)$Se_2$ thin-film solar cells using *wx*AMPS. Optik. 2016;127(1):182.
[11] Heriche H, Rouabah Z, Bouarissa N. High-efficiency CIGS solar cells with optimization of layers thickness and doping. Optik. 2016;127(24):11751.
[12] Fonash S, Arch J, Cuiffi J, et al. A manual for AMPS-1D for windows 95/NT. The center for nanotechnology education and utilization. University Park: The Pennsylvania State University; 1997.
[13] Degrave S, Burgelman M, Nollet P. Modelling of polycrystalline thin film solar cells: new features in SCAPS version 2.3. 3rd World Conference on Photovoltaic Energy Conversion, Osaka-Japan, 2003: 487.
[14] Armstrong JC, Cui JB, Chen TP. ALD processed MgZnO buffer layers for Cu(In,Ga)$S_2$ solar cells. 40th

IEEE Photovoltaic Specialist Conference, Denver (Colorado) USA, 2014: 304.
[15] Gray J, Wang X, Chavali RVK, et al., 2015, "ADEPT 2.1", [cited 2020 Sep 09]. https://nanohub.org/resources/adeptnpt
[16] Mostefaoui M, Mazari H, Khelifi S, et al. Simulation of high efficiency CIGS solar cells with SCAPS-1D software. Enrgy Proced. 2015;74:736.
[17] Asaduzzaman M, Hosen MB, Ali MK, et al. Non-toxic buffer layers in flexible Cu(In, Ga)$Se_2$ photovoltaic cell applications with optimized absorber thickness. Int J Photoenergy. 2017;2017:4561208.
[18] Bauer A, Sharbati S, Powalla M. Systematic survey of suitable buffer and high resistive window layer materials in $CuIn_{1-x}Ga_xSe_2$ solar cells by numerical simulations. Sol Energ Mat Sol C. 2017;165:119.
[19] Bouchama I, Boudour S, Bouarissa N, et al. Quantum and conversion efficiencies optimization of superstrate CIGS thin-films solar cells using $In_2Se_3$ buffer layer. Opt Mater. 2017;72:177.
[20] Hariskos D, Spiering S, Powalla M. Buffer layers in Cu(In,Ga)$Se_2$ solar cells and modules. Thin Solid Films. 2005;99:480–481.
[21] Lee CS, Larina L, Shin YM, et al. Design of energy band alignment at the $Zn_{1-x}Mg_xO$/Cu(In,Ga)$Se_2$ interface for Cd-free Cu(In,Ga)$Se_2$ solar cells. Phys Chem Chem Phys. 2012;14(14):4789. .
[22] Hadjab M, Berrah S, Abid H, et al. First-principles investigation of the optical properties for rocksalt mixed metal oxide $Mg_xZn_{1-x}O$. Mater Chem Phys. 2016;182:182.
[23] Pettersson J, Platzer-Björkman C, Zimmermann U, et al. Baseline model of graded-absorber Cu(In,Ga)$Se_2$ solar cells applied to cells with $Zn_{1-x}Mg_xO$ buffer layers. Thin Solid Films. 2011;519(21):7476. .
[24] Pandey SK, Mukherjee S. Device modeling and optimization of high-performance thin film CIGS solar cell with $Mg_xZn_{1-x}O$ buffer layer. 5th IEEE International Nanoelectronics Conference, Singapore, 2013: 353
[25] Pandey SK. Enhanced performance and defect analysis of MgZnO based CIGS solar cell. J Nanoelectron Optoelectron. 2016;11(5):649.
[26] Liu Y, Sun Y, Rockett A. A new simulation software of solar cells–*wx*AMPS. Sol Energ Mater Sol C. 2012;98:124.
[27] Parisi A, Curcio L, Rocca V, et al. Thin film CIGS solar cells, photovoltaic modules, and the problems of modeling. Int J Photoenergy. 2013;2013:817424.
[28] Zhu H, Kalkan AK, Hou J, et al. Applications of AMPS-1D for solar cell simulation 15th National center for photovoltaics program review meeting, AIP Conference Proceedings, 1999;462:309.
[29] Boudour S, Bouchama I, Bouarissa N, et al. A study of CdTe solar cells using Ga-doped $Mg_xZn_{1-x}O$ buffer/TCO layers: simulation and performance analysis. J Sci Adv Mat Dev. 2019;4:111.
[30] Boudour S, Bouchama I, Hadjab M, et al. Optimization of defected ZnO/Si/$Cu_2O$ heterostructure solar cell. Opt Mater. 2019;98:109433.
[31] Yaşar S, Kahraman S, Çetinkayaa S, et al. Numerical thickness optimization study of CIGS based solar cells with *wx*AMPS. Optik. 2016;127(20):8827.
[32] Omer BM, Pivrikas A, Mohamed AK. AMPS-1D modeling of P3HT/PCBM bulk heterojunction solar cell. 37th IEEE Conference Photovoltaic Specialists Conference, Seattle (Washington) USA, 2011, 2: 734
[33] Dabbabi S, Ben Nasr T, Turki NK. Parameters optimization of CIGS solar cell using 2D physical modeling. Results Phys. 2017;7:4020.
[34] Moon MMA, Rahman MF, Hossain J. Comparative study of the second generation a-Si: H,CdTe, and CIGS thin-film solar cells. Adv Mat Res. 2019;1154:1662.
[35] Asaduzzaman M, Bahar AN, Bhuiyan MMR. Dataset demonstrating the modeling of a high performance Cu(In,Ga)$Se_2$ absorber based thin film photovoltaic cell. Data Brief. 2017;11:296.
[36] Nakada T. CIGS-based thin film solar cells and modules: unique material properties. Electron Mater Lett. 2012;8(2):179.
[37] Busacca AC, Rocca V, Curcio L, et al. Parametrical study of multilayer structures for CIGS solar cells. 3rd International Conference on Renewable Energy Research and Applications, Milwaukee - USA, 2014: 964.
[38] Gloeckler M, Fahrenbruch AL, Sites JR. Numerical modeling of CIGS and CdTe solar cells: setting the baseline. 3rd World Conference on Photovoltaic Energy Conversion, Osaka - Japan, 2003: 491.
[39] Gloeckler M. Numerical modeling of CIGS solar cells: definition of the baseline and explanation of superposition failure. Thesis, Colorado State University Fort Collins, Colorado, 2003
[40] Touafek N, Mahamdi R. Excess defects at the CdS/CIGS interface solar cells. Chalcogenide Lett. 2014;11(11):589.
[41] Bechlaghem S, Zebentout B, Benamara Z. Investigation of Cu(In, Ga)$Se_2$ solar cell performance with non-cadmium buffer layer using TCAD-SILVACO. Mat Sci-Poland. 2018;36(3):514.